https://ntrs.nasa.gov/search.jsp?R=19770018765 2020-03-22T09:51:15+00:00Z

General Disclaimer

One or more of the Following Statements may affect this Document

- This document has been reproduced from the best copy furnished by the organizational source. It is being released in the interest of making available as much information as possible.

- This document may contain data, which exceeds the sheet parameters. It was furnished in this condition by the organizational source and is the best copy available.

- This document may contain tone-on-tone or color graphs, charts and/or pictures, which have been reproduced in black and white.

- This document is paginated as submitted by the original source.

- Portions of this document are not fully legible due to the historical nature of some of the material. However, it is the best reproduction available from the original submission.

Produced by the NASA Center for Aerospace Information (CASI)

X-695-77-40

TMX 71323

RELATIONSHIP BETWEEN AURORAL SUBSTORMS AND THE OCCURRENCE OF TERRESTRIAL KILOMETRIC RADIATION

(NASA-TM-X-71323) RELATIONSHIP BETWEEN AURORAL SUBSTORMS AND THE OCCURRENCE OF TERRESTRIAL KILOMETRIC RADIATION (NASA) 15 p HC A02/MF A01 CSCL 04A

N77-25709

Unclas G3/46 35253

M. L. KAISER
J. K. ALEXANDER

JUN 1977
RECEIVED
NASA STI FACILITY
INPUT BRANCH

MARCH 1977

GSFC — GODDARD SPACE FLIGHT CENTER —
GREENBELT, MARYLAND

RELATIONSHIP BETWEEN AURORAL SUBSTORMS AND THE OCCURRENCE OF TERRESTRIAL KILOMETRIC RADIATION

M. L. Kaiser and J. K. Alexander
NASA/Goddard Space Flight Center
Laboratory for Extraterrestrial Physics
Planetary Sciences Branch
Greenbelt, Maryland 20771

ABSTRACT

We have examined the correlation between magnetospheric substorms as inferred from the AE(11) index and the occurrence of terrestrial kilometric radiation (TKR) as observed by the Goddard radio astronomy experiment onboard the IMP-6 spacecraft. In general, we find that AE and TKR are well correlated when observations are made from above the 15-03 hr local time zone and are rather poorly correlated over the 03-15 hr zone. High-resolution dynamic spectra obtained during periods of isolated substorms indicate that low-intensity, high-frequency TKR commences at about the same time as the substorm growth phase. The substorm expansion phase corresponds to a rapid intensification and bandwidth increase of TKR. When combined with our previous results, these new observations imply that many TKR events begin at low altitudes and high frequencies ($\sim$ 400-500 kHz) and spread to higher altitudes and lower frequencies as the substorm expands.

Several authors (Benediktov et al., 1968; Dunckel et al., 1970; Gurnett, 1974; Kaiser and Alexander, 1977) have shown that the intense magnetospheric radio emissions known as terrestrial kilometric radiation (TKR) or auroral kilometric radiation (AKR) are correlated both in occurrence and in intensity with magnetospheric substorms as indicated by the auroral electrojet index (AE). In the most detailed study to date, Voots et al. (1977) showed that TKR can be a very reliable indicator of auroral disturbances since TKR power flux density and AE are well correlated on a coarse time scale ($\geq$ 1 hr). In this report we confirm those findings and we investigate some of the finer scale temporal aspects of this relationship in order to determine the detailed time correlation between substorm growth and expansion phases and the development of TKR activity.

OBSERVATIONS

In our investigation of the correlation between TKR and substorm activity we have used dynamic spectra of the magnetospheric radio emissions obtained with the Goddard Space Flight Center radio astronomy experiment on IMP-6 between April 20, 1971, and September 26, 1972. That experiment was comprised of a pair of step-frequency receivers connected to a 91-m dipole antenna to provide spectral scans at 39 discrete channels between 30 kHz and 9.1 MHz every 5.1 sec. In Figure 1 we compare dynamic spectral displays of the IMP-6 measurements and plots of the AE(11) index for four separate days. In each 24-hr dynamic spectrum we have used 10-min averages of intensity, and darkness is proportional to intensity. The corresponding 24-hr plots of AE(11) at 2.5-min intervals are shown immediately below each dynamic spectrum.

The examples in Figures 1a and 1b show a very good correlation between TKR activity at frequencies between ~ 100 and 500 kHz and variations in AE. There are conspicuous radio noise events between 03 and 09 hr UT and 16 and 21 hr UT on 19 September 1971 and between 12 and 24 hr UT on 12 October 1971 that are associated with large increases in the AE index during the same intervals. In addition, there are distinct TKR events centered at about 1130 UT on 19 September 1971 and 0400 on 12 October 1971 that are possibly associated with relatively minor, simultaneous enhancements in AE. Notice also that the rather abrupt onsets in AE enhancements at approxiamtely 0230 and 1600 UT on 19 September 1971 and 1230 and 1530 UT on 12 October 1971 coincide with comparable TKR onsets to within ± 20 min.

In Figures 1c and 1d, we have two examples of remarkably poor correlation between TKR activity and the AE index. Two large substorms (AE > 600) occurred on 23 March 1972, and yet there is no substantial kilometer wavelength emission associated with the AE enhancements. Instead all that we observe in the IMP-6 data are a few relatively weak type III solar radio bursts (e.g. at 05 to 10 hr UT). In Figure 1d we see the intense kilometric activity in the first half of 13 September 1971, but during the very large storm apparent in the AE plot after 1230 UT the radio data are moderately elevated but lack any distinct signature characteristic of TKR events.

In order to make a qualitative assessment of the correlation between TKR activity and substorm activity as a function of subsatellite local time, we have made an orbit-by-orbit comparison of IMP-6 dynamic spectral data and AE. Although not

quantitatively rigorous, such visual comparisons of TKR and AE variations can very easily identify and compensate for competing effects in the radio data such as solar bursts. For each 4.18-day orbit, we compared dynamic spectra and AE plots for the 3-day period centered on the time of apogee and assigned a relative "correlation weight" ranging between 0 (poor correlation with AE) to 6 (very good correlation) for that orbit. Figures 1a and 1b are examples of days from orbits with high correlation weights, and Figures 1c and 1d are examples of days from orbits with low relative correlation weights. Radio data from the perigee segments of each orbit were not used since obscuration of TKR by the plasmasphere and locally generated noise events are likely to impede reliable comparisons between TKR measurements and AE.

In Figure 2 we have plotted the variation of relative correlation weight for each IMP-6 orbit as a function of the subsatellite MLT at apogee. Each vertical bar represents the correlation of TKR dynamic spectra with AE for one orbit plotted relative to a weight of 3 ("fair" correlation). Orbits that have been assigned a weight below 3 are defined (for our purposes) to be poorly correlated with substorm activity whereas orbits assigned a weight above 3 are said to be well correlated with substorm activity. Notice from Figure 2 that we tend to find good correlation between about 15 hr and 03 hr MLT and rather poor correlation in the 03-15 hr MLT hemisphere. In other words, AE and TKR are well correlated when we are in the main beam of the TKR radiation pattern (defined as 16 hr - 04 hr MLT by Alexander and Kaiser, 1976) and are often poorly correlated when observations are obtained outside

the TKR beam. This finding agree well with the results presented by Voots et al. (1977) who correlated the AE index with a single frequency channel at 178 kHz.

The examples of good AE-TKR correlation in Figures 1a and 1b correspond to observations obtained when IMP-6 was in the main beam of the TKR radiation pattern. The subsatellite MLT was between 01 and 02 hr on 19 September 1971 and between 22 and 23 hr on 12 October 1971, and so the high degree of correlation is consistent with our interpretation of Figure 2. On 23 March 1972 (Figure 1c) the subsatellite MLT was between 12 and 13 hr, and therefore not in the main TKR beam, so that the correlation between TKR and AE was less likely to be positive. The event of 13 September 1972 (Figure 1d) is apparently an anomaly. The location of the IMP-6 spacecraft was nearly identical to the 19 September 1971 (Figure 1a) example. However, a sudden commencement geomagnetic storm (K_p = 8) began at 1240 UT on 13 September and continued into the next day. We do find TKR associated with the sharp sudden commencement, but the dynamic spectral properties of the emission after 1400 UT are certainly not typical of TKR events. It is possible that the source region moved either to lower altitude or lower latitude during the substorm expansion phase so that the plasmasphere obscured our line-of-sight to the source; however, this is pure speculation.

We have examined our high time resolution data (5.1 sec/scan) to determine, for isolated substorms, the details of TKR onset times. The period from mid-August to mid-February each year corresponds to times when the IMP-6 subsatellite point was in the 15-03 hr hemisphere for most of each orbit. During these periods, we identified 29 isolated

substorms from the AE(11) index. We used only those events which were preceded by a period of several hours of very quiet conditions (AE < 50). Initial efforts using TKR intensities from only one receiver channel quickly showed that apparently no single narrow-band frequency channel can be used to completely characterize the TKR morphology. Occasions exist when TKR consists of very narrow-banded emission (half power band width ~ 100 kHz) centered from as high as 500 kHz to as low as perhaps 100 kHz. These events, or portions of events, are easily "missed" by a single isolated frequency channel. Therefore, in this study we have used our entire frequency band on IMP-6 which includes at least ten channels in the TKR band. Figure 3 shows four examples of relatively isolated substorms with the IMP-6 dynamic spectra displayed on the same 6-hour time grids. The trend evident in these four events as well as most of our other examples is for the initial or growth phase of the substorm to coincide with relatively weak, narrow-banded TKR emission. The substorm expansion phase corresponds to a rapid TKR intensification and to an increase in bandwith.

Figure 3 also suggests that substorm associated TKR events begin at high-frequencies (400-500 kHz) and expand to lower frequencies as AE increases. We have investigated this important observation further by conducting digital cross-correlation analyses between 6-hour intervals of the AE(11) index and the received power on each IMP-6 frequency channel from 110 kHz to 475 kHz. For those 6-hour intervals with correlation coefficients of 0.5 or more (40-50% of all 6-hour intervals in the 15-03 hr local time zone), the maximum correlation is achieved with TKR leading AE progressively more and more with

ascending observing frequency. At 475 kHz, approximately twice as many 6-hour intervals have correlation coefficients > 0.5 for TKR leading AE by 10 to 50 minutes than for AE preceeding TKR. The best correlations at the higher TKR frequencies seems to occur with TKR preceeding AE by about 10 minutes. In the range from 185 to 292 kHz, corresponding to the center of the TKR band, the best correlations are achieved with no offset between TKR intensities and AE index. At lower frequencies (110-155 kHz), best correlations occur with either no offset or with AE preceeding TKR by 10-20 minutes. Thus it appears that the trend suggested by the examples in Figure 3 and other similar displays is, in fact, a general morphological feature of substorm related TKR.

SUMMARY AND DISCUSSION

The qualitative visual comparison between dynamic spectral displays and plots of the AE index, and the quantitative cross-correlation between TKR received power and AE index are in good general agreement as to the relationship between TKR and auroral substorms. We find that:

1) TKR and AE are better correlated in the 15-03 hr hemisphere than in the 03-15 hr hemisphere in excellent agreement with the findings of Voots et al. (1977). When observations are made from over the 15-03 hr hemisphere even small changes in AE are reflected in the TKR intensity, but over the opposite hemisphere only large excursions in AE are accompanied by TKR emission. We believe the apparent differences between these two hemispheres simply evolves from the TKR "beam pattern" as discussed by Gurnett (1974), Alexander and Kaiser (1977), and Green et al. (1977) rather than any physically different mechanisms.

2) When relatively isolated events are examined, the detailed correlation between TKR and auroral substorms appears to be quite good. Low-intensity TKR often commences at the high-frequency end of the TKR band at the start of a substorm growth phase and subsequent large increases in TKR intensity and bandwidth coincide with the substorm expansion phase. This differs with the findings of Voots et al. (1977) who state that "the detailed short time scale (< 1 hour) intensity variations often do not have a close association with variations in the AE index". We believe this difference may result from the use by Voots and colleagues of only a single frequency channel to monitor TKR. The narrow-banded high-frequency TKR which often exists during the substorm growth phase could very easily be "missed" by the single channel at 178 kHz. Also, the Iowa receiver threshold at 178 kHz appears, from Figures 1 and 2 of Voots et al. (1977), to be 1-2 x 10^{-20} Wm^{-2} Hz^{-1}, whereas the Goddard experiment can detect cosmic background at $\sim 10^{-22}$ Wm^{-2} Hz^{-1} at 185 kHz. This may mean that low-intensity TKR was not detected by the Iowa experiment.

The high-to-low frequency progression of TKR events is consistent with our previous results (Kaiser and Alexander, 1977) that the frequency of peak TKR flux, f_o, decreases as AE increases. During the substorm growth phase, AE is low and f_o is high. During the expansion phase when AE increases rapidly, the TKR bandwidth widens primarily toward lower frequencies so that f_o is lower.

The high-to-low frequency trend becomes particularly intriguing when combined with the findings of Alexander and Kaiser (1976) that

high frequency TKR appears to emanate closer to the earth than low frequency TKR. At least two possible explanations for this observed phenomenology come to mind. It could be that the high-to-low frequency trend results from wave propagation effects. During the early portion of the substorm TKR is generated at low altitude and we may only be able to see the high-frequency end of the TKR band because the lower frequencies may be obscured by the plasmasphere. This would be consistent with the findings of Green et al. (1977) that, in general, high TKR frequencies have a wider beam pattern than lower frequencies. As the substorm progresses, the lower TKR frequencies become visible because the plasmasphere has contracted in size or the source region has expanded upward into regions of lower plasma density where the beam pattern of TKR would be broader.

Another possibility is that the physical mechanism responsible for TKR preferentially emits at high frequencies during the initial minutes of a substorm. As particle precipitation increases and the plasmasheet greatly expands in volume, the mechanism is able to produce TKR over a larger bandwidth and altitude range.

No doubt other viable explanations exist that describe the observed behavior of TKR during substorms, and additional efforts in this area may well lead to an understanding of the TKR emission mechanism.

ACKNOWLEDGEMENTS

The authors thank Drs. P. Rodriguez, D. Fairfield, M. Caan and N. Ness for useful comments and discussions.

REFERENCES

Alexander, J.K. and M.L. Kaiser, Terrestrial kilometric radiation, 1, Spatial structure studies, J. Geophys. Res., 81, 5948, 1976.

Benediktov, E.A., G.G. Getmantsev, N.A. Mityakov, V.O. Papoport, and A.F. Tarasov, Relation between geomagnetic activity and the sporadic radio emission recorded by the electron satellites, Kosm. Issled., 6, 1.

Dunckel, N., B. Ficklin, L. Rorden, and R.A. Helliwell, Low-frequency noise observed in the distant magnetosphere with OGO 1, J. Geophys. Res., 75, 1854, 1970.

Green, J.L., D.A. Gurnett, and S.D. Shawhan, The angular distribution of auroral kilometric radiation, J. Geophys. Res., in press, 1977.

Gurnett, D.A., The earth as a radio source: Terrestrial kilometric radiation, J. Geophys. Res., 79, 4227, 1974.

Kaiser, M.L. and J.K. Alexander, Terrestrial kilometric radiation, 3, Average spectral properties, J. Geophys. Res., in press, 1977.

Russell, C.T., The solar wind and magnetospheric dynamics, in Corelated Interplanetary and Magnetospheric Observations, edited by D.E. Page, p. 3, D. Reidel, Dordrecht, Netherlands, 1974.

Voots, G.R., D.A. Gurnett, and S. -I. Akasofu, Auroral kolometric radiation as an indicator of auroral magnetic disturbances, J. Geophys. Res., in press, 1977.

FIGURE CAPTIONS

Figure 1. Four examples of TKR-AE correlation. The top frame of each panel is a dynamic spectral display with increasing darkness proportional to increasing intensity. The corresponding 24-hr plots of AE are shown immediately below each dynamic spectrum.

Figure 2. Qualitative correlation coefficient as a function of sub-satellite local time. Displays like Figure 1 were examined visually and assigned a number for each day ranging from 6 for days with excellent correlation to 0 for poor correlation.

Figure 3. Four examples of relatively isolated excursions in the AE(11) index with the corresponding IMP-6 dynamic spectra displayed on the same 6-hr time grid. All four examples show that the slow rise in AE denoting a substorm growth phase is accompanied by relatively low-intensity TKR primarily at the high end of the TKR band. The rapid increase in AE corresponding to the substorm expansion phase coincides with bandwidth and intensity increases in the TKR.

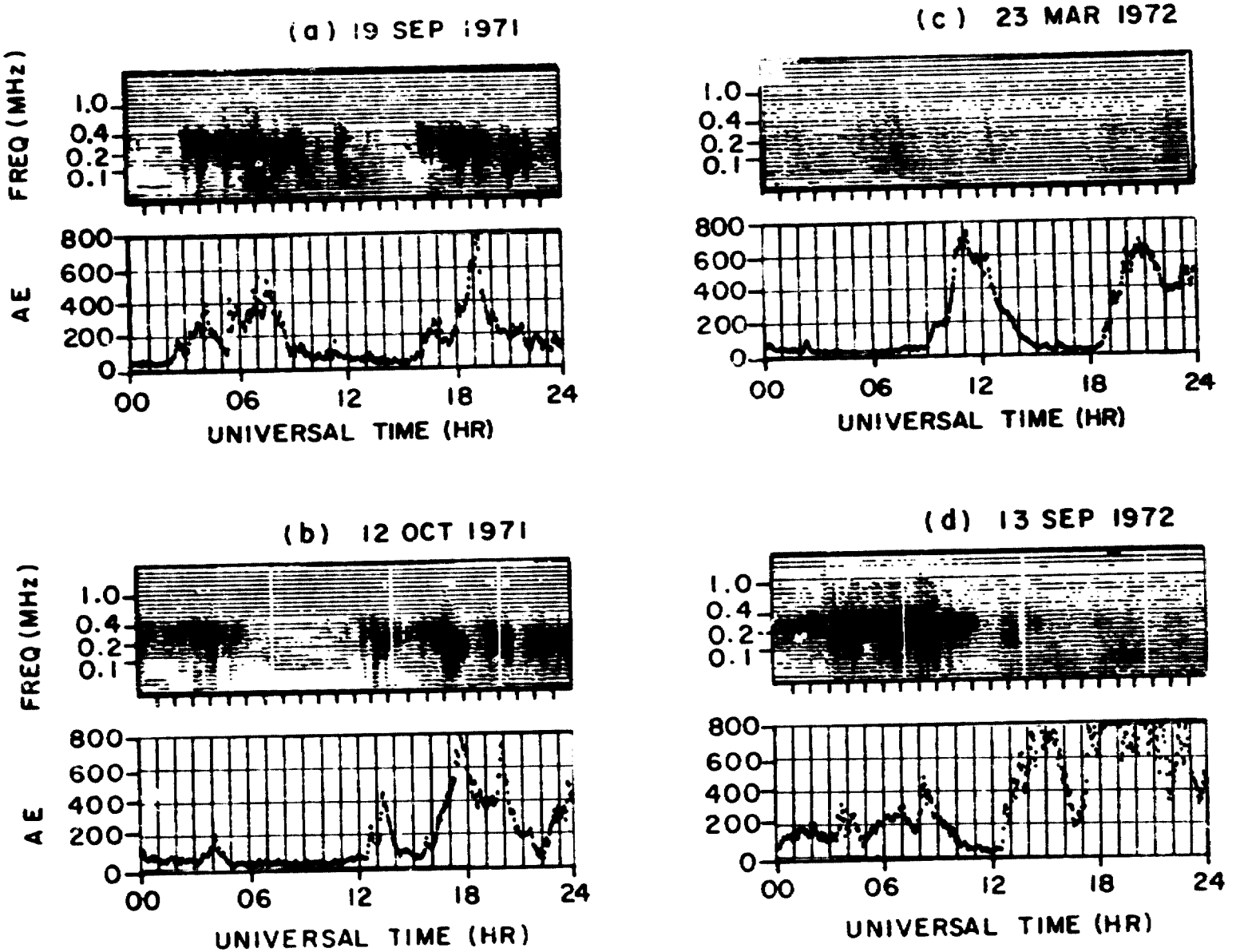

Fig. 1

REPRODUCIBILITY OF THE

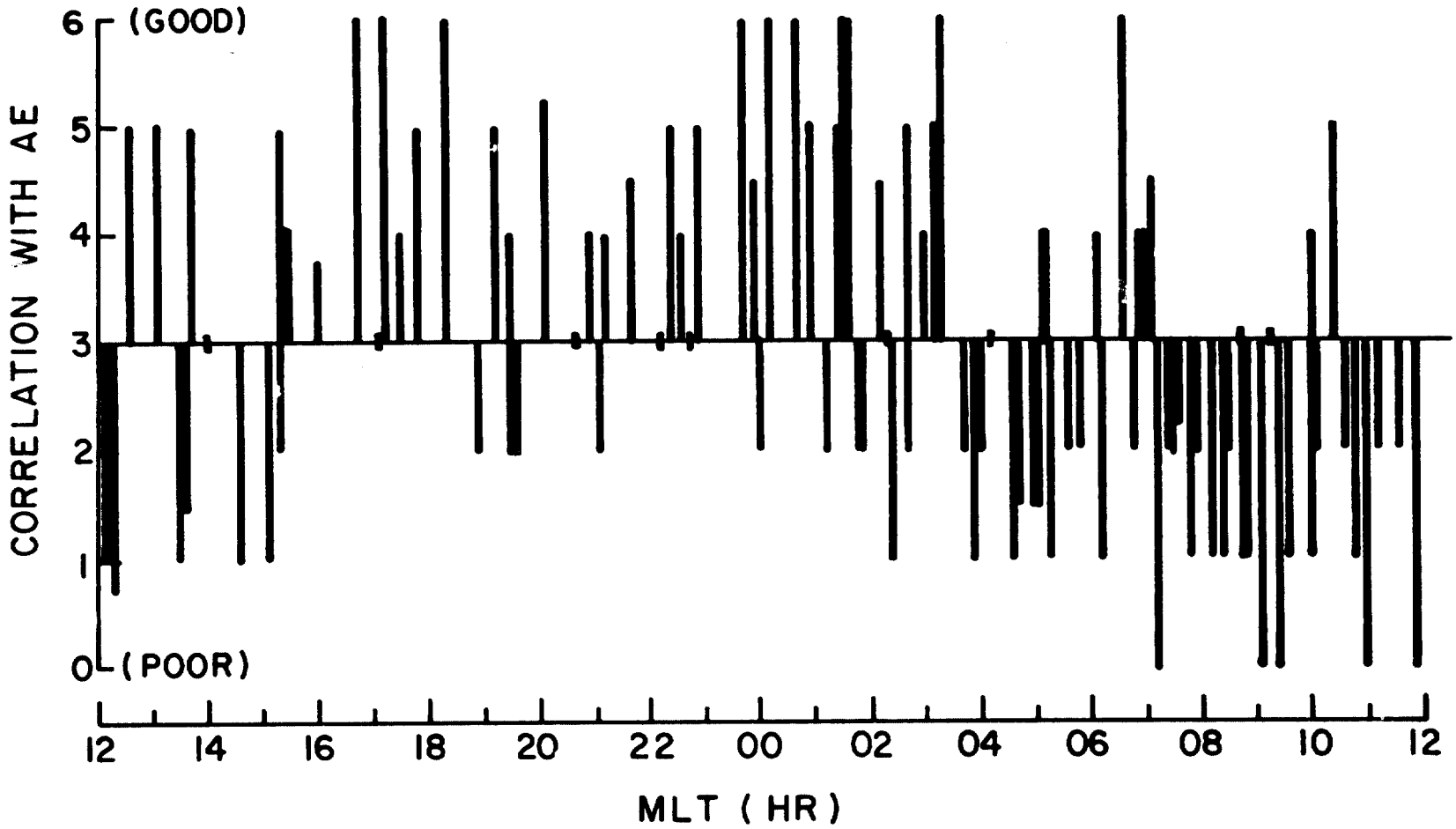
6 (GOOD)
5
4
3
2
1
0 (POOR)
CORRELATION WITH AE
12
14
16
18
20
22
00
02
04
06
08
10
12
MLT (HR)

Fig. 2

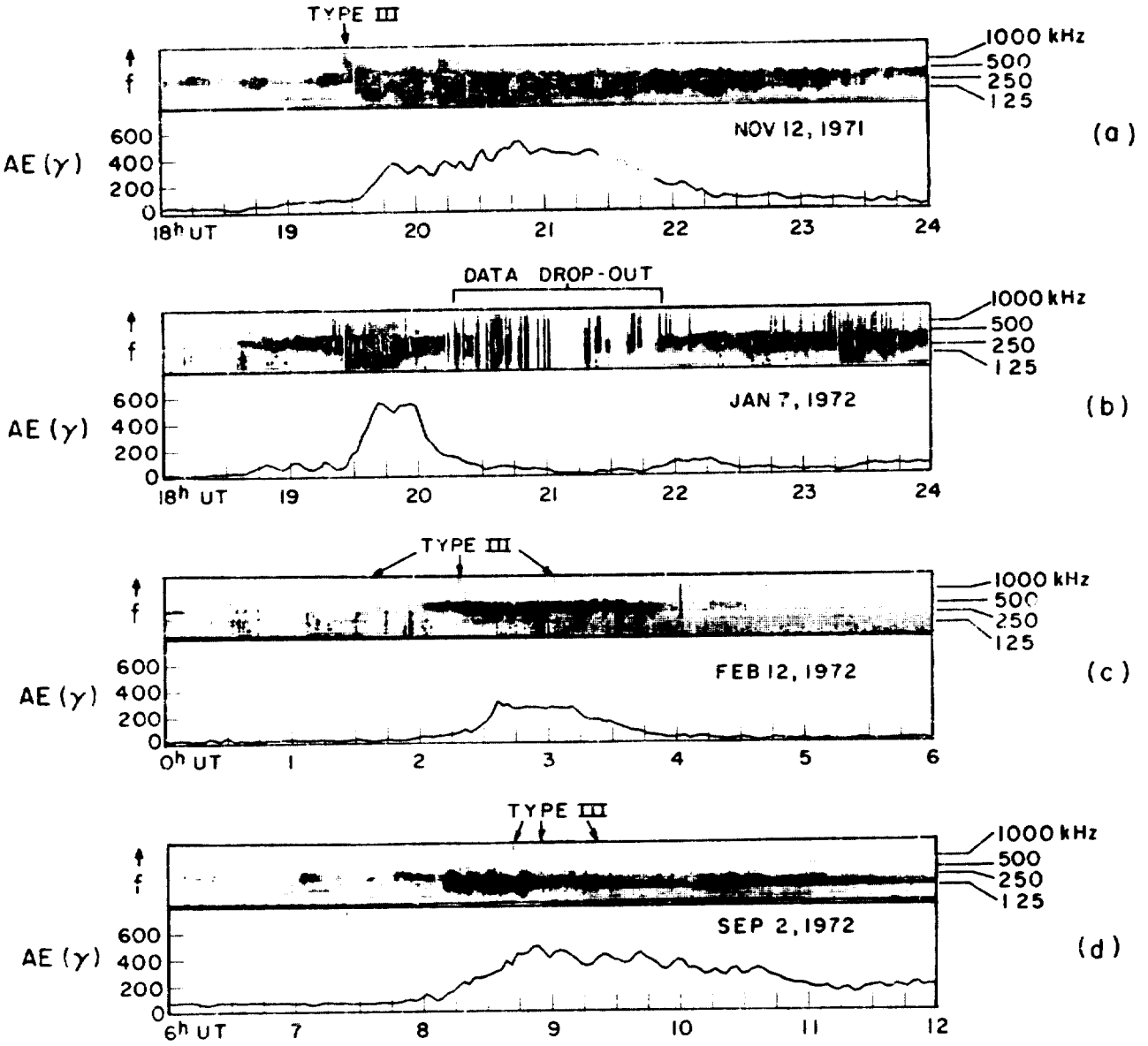
TYPE III
1000 kHz
500
250
125
f
NOV 12, 1971
AE (γ)
600
400
200
0
18h UT
19
20
21
22
23
24
(a)
DATA DROP-OUT
JAN 7, 1972
(b)
FEB 12, 1972
0h UT
1
2
3
4
5
6
(c)
SEP 2, 1972
6h UT
7
8
9
10
11
12
(d)

Fig. 3